Ion Upflow Dependence on Ionospheric Density and Solar Photoionization

Marc Lessard[1], Ian Cohen[1,2], Roger Varney[3], Kjellmar Oksavik[4,5], Matt Zettergren[6], Kristina Lynch[7]

[1]UNH, [2]JHU/APL, [3]SRI International, [4]University of Bergen, [5]UNIS, [6]ERAU, [7]Dartmouth

2015 AGU Fall Meeting, SM23B-2562

Introduction

Ionospheric plasma (particularly O^+) added into the tail via ion outflow can alter the reconnection rate and affect a range of magnetospheric processes. Furthermore, *Lessard et al.* [2015] showed that EMIC wave frequencies depend on heavy ions and exhibit a solar cycle dependence.

"Ion outflow" of light thermal ions (H^+, He^+) and light and heavy energized ions (H^+, He^+, O^+, N^+, NO^+, O_2^+, N_2^+) can be attributed to multiple processes occurring in the polar and auroral ionosphere. However, with the exception of H^+, these ions require a secondary energization source to achieve escape velocity. This distinguishes between *"ion upflow"* processes, which initially move ions to higher altitudes, and secondary *"ion outflow"* processes that energize ions to escape velocities.

Wahlund et al. [1992] first separated TUI into two types: thermal plasma upflows (Type-1) and upflow due to enhanced field-aligned electric fields (Type-2). This study specifically focuses on Type-2 upflow, which is believed to result from a vertical ambipolar electric field created by the deposition of energy from soft electron precipitation.

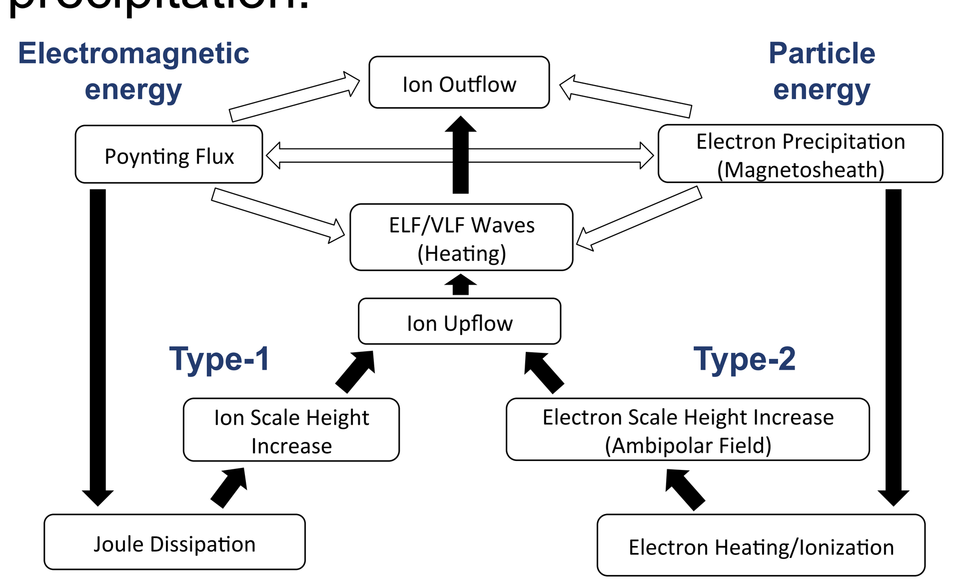

Figure 1. Adapted from *Strangeway et al.* [2005], this figure breaks down the two types of ion upflow based on the flow of energy. It also underscores the secondary processes (here WPI) that are necessary to achieve escape velocities, hence differentiating ion upflow from ion outflow.

Model Description

The single field line ionosphere/polar wind model introduced by Varney et al. [2014] solves the dynamics of thermal ions, thermal electrons, and suprathermal electrons on a single open field line between 97 and 6300 km altitude. Here, to model a discrete auroral arc in the simulations presented here assume a Maxwellian distribution with a characteristic energy of 800 eV accelerated through a field-aligned potential drop.

Initial conditions were obtained by running the model for 48 h prior without precipitation. To investigate the effect of ionospheric density on upflow, these precursor runs were performed using six different $F_{10.7}$ values ranging from 70 to 120 in the solar EUV model. Figure 2 shows the electron density profiles from the end of these six long runs. Run 4 ($F_{10.7}$=100) produced a peak F electron density similar to that observed by the Poker Flat Incoherent Scatter Radar (PFISR) observations during the MICA launch. The runs presented here introduce 360 s of "auroral" precipitation into the quasi-equilibrium state of the model established by the 48 h precursor runs.

Model Results

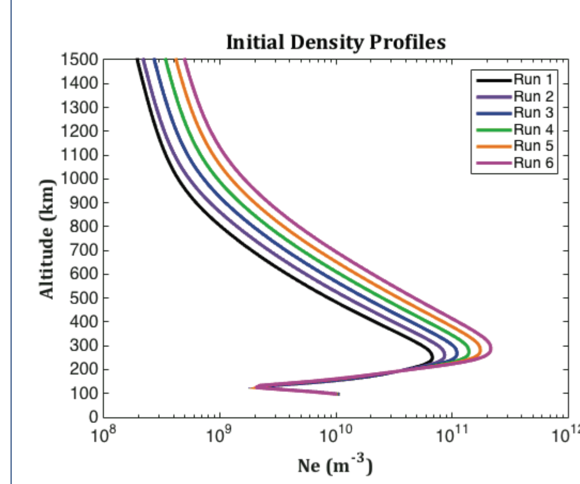

Figure 2. Initial ionospheric density profiles for the six simulation runs.

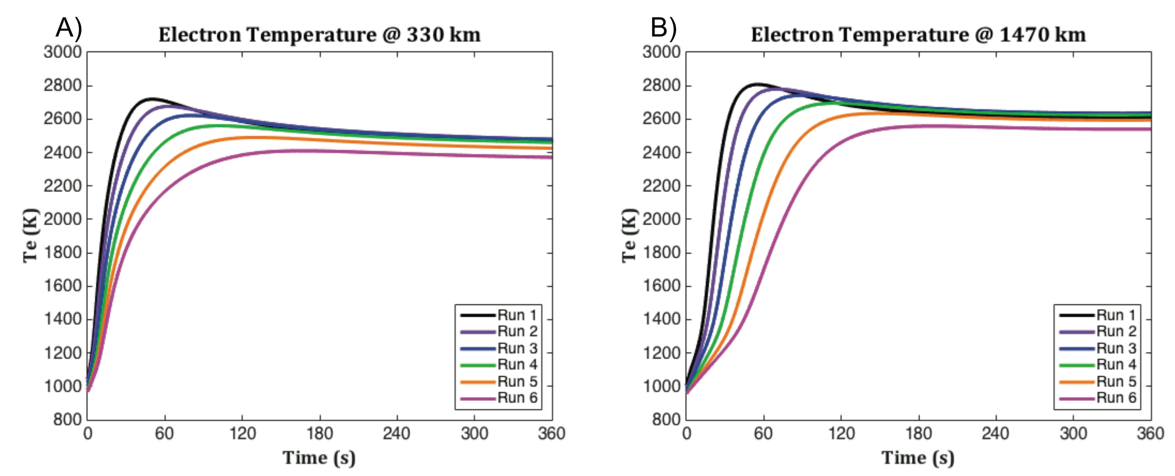

Figure 3. Simulation results of the electron temperature evolution during the period of precipitation at 300 and 1470 km, respectively. The colors correspond to the runs of varying ionospheric density, as shown in Figure 2.

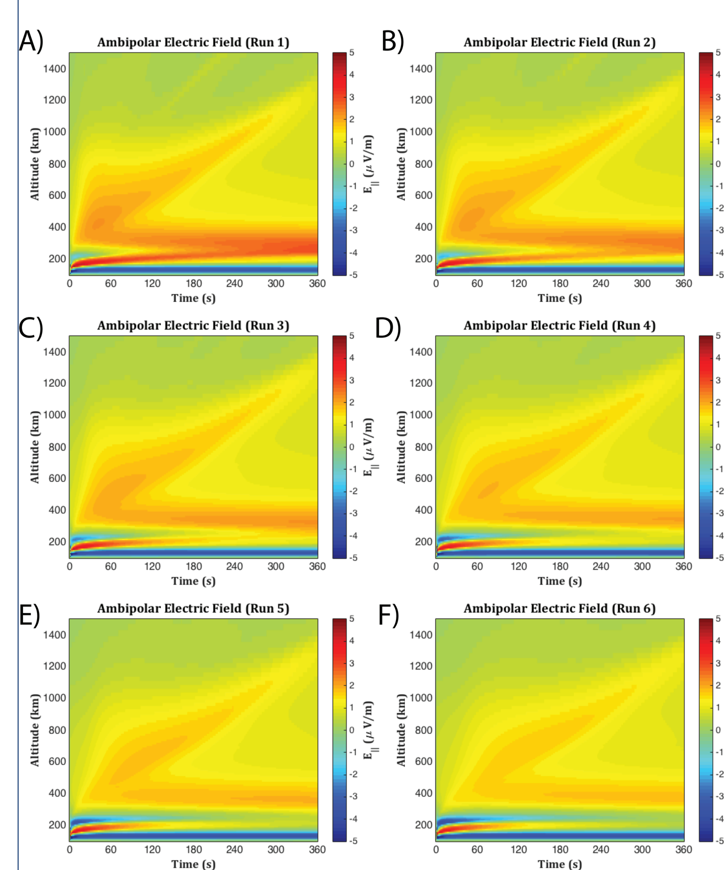

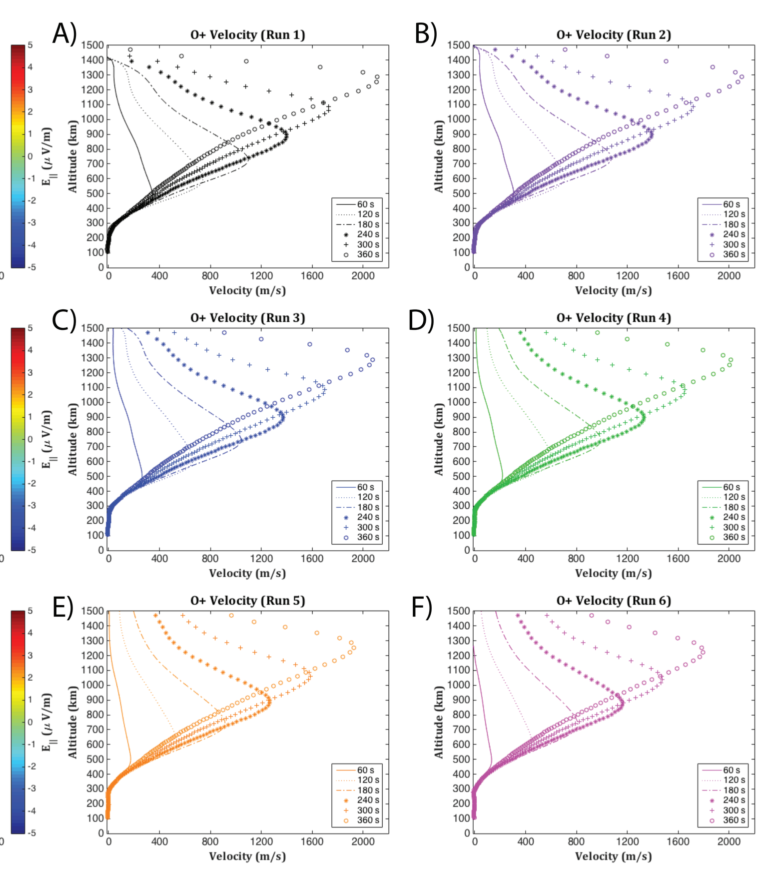

Figure 4 (far left) shows simulation results of the strength of the field-aligned ambipolar electric field versus altitude over time. It clearly shows that the field weakens in runs with higher ionospheric density. **Figure 6** (left) shows the evolution of the O^+ upflow velocity at 1-min intervals during the precipitation. The colors correspond to initial ionospheric density profiles shown in Figure 2.

The simulation was able to generate realistic upflows in response to the precipitation, with all of the characteristics indicative of Type-2. Most importantly it generated enhanced electron temperatures (see Figure 3). Although much heating was not seen at very high altitudes, two effects of enhanced ionospheric density were apparent: decreased electron temperatures and longer heating timescales.

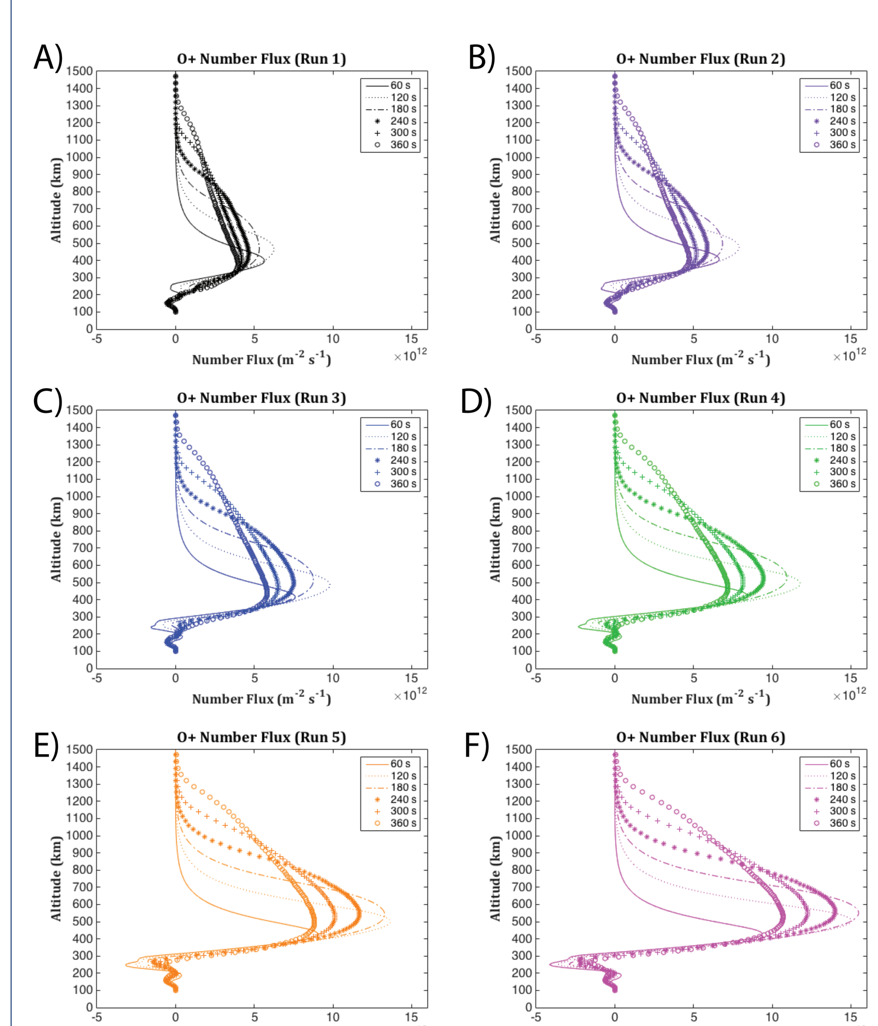

Figure 7 (above) shows the evolution of the O+ upflow flux at 1 minute intervals during the precipitation period. The colors correspond to initial ionospheric density profiles shown in Figure 2.

However, despite the weakened ambipolar field and lower upflow velocities, the simulations still show enhanced ion fluxes in runs with enhanced ionospheric density (Figure 7). This is most likely due to the fact that there are more ions present to be accelerated.

The simulations also showed that enhanced ionospheric density decreases the strength of the field-aligned ambipolar electric field, which plays an important role in the acceleration of ions in the Type-2 upflow process. Subsequently, the weakened ambipolar field results in lower upflow velocities in runs with higher ionospheric density.

The Role of Solar Photoionization

The simulations show that ionospheric density can affect ion upflow, so what can affect ionospheric density?

Solar photoionization!

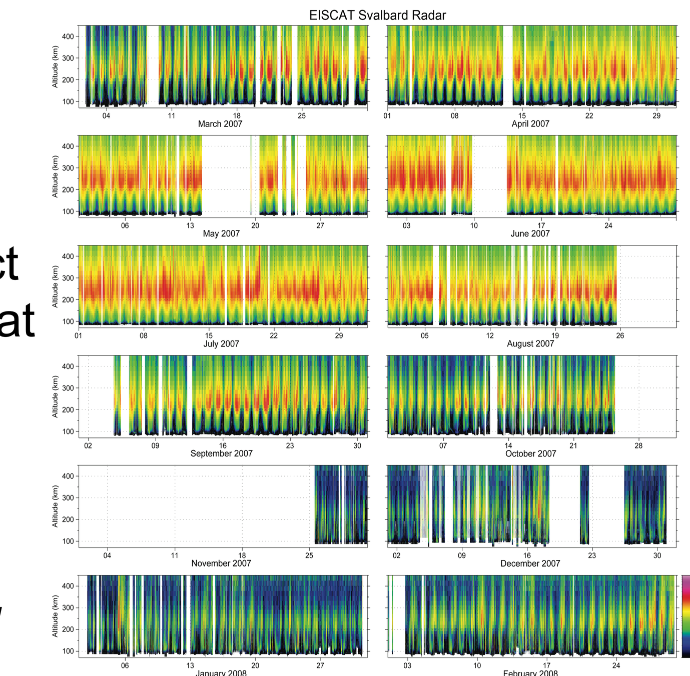

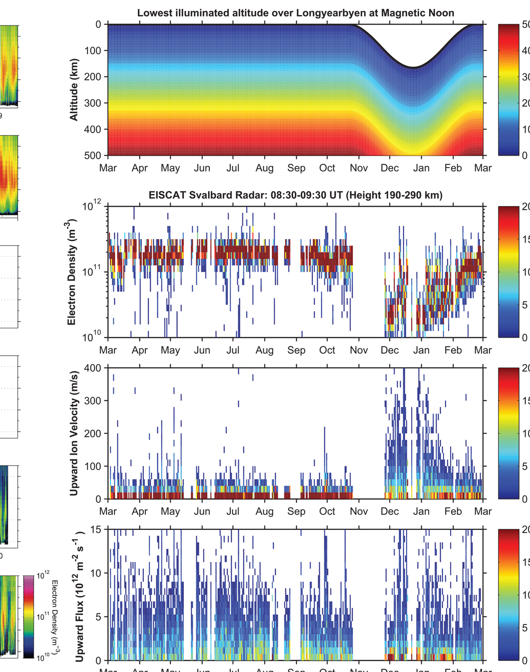

Figure 8 (above, left) shows data from the EISCAT Svalbard radar during the International Polar Year (IPY) clearly showing the seasonal (order of magnitude) increase in ionospheric density during the summer. **Figure 9** (above, right) shows IPY data supporting the results of the simulations presented here. The observations clearly show decreased upflow velocities and increased fluxes during the summer when electron density is enhanced due to solar photoionization.

Conclusions

A new simulation based on the model of *Varney et al*. [2014] was run for six cases with peak ionospheric density varying from 6.8×10^{10} to 2.16×10^{11} m^{-3}.

The simulation results generated realistic ion upflows in response to the auroral precipitation, generating electron temperatures in good agreement with rocket observations at F region altitudes.

The simulations demonstrate that enhanced ionospheric density yields:

- Lower ionospheric T_e
- Longer heating timescales
- Weaker ambipolar electric field
- Lower ion upflow velocities
- Longer upflow timescales
- Larger ion upflow fluxes

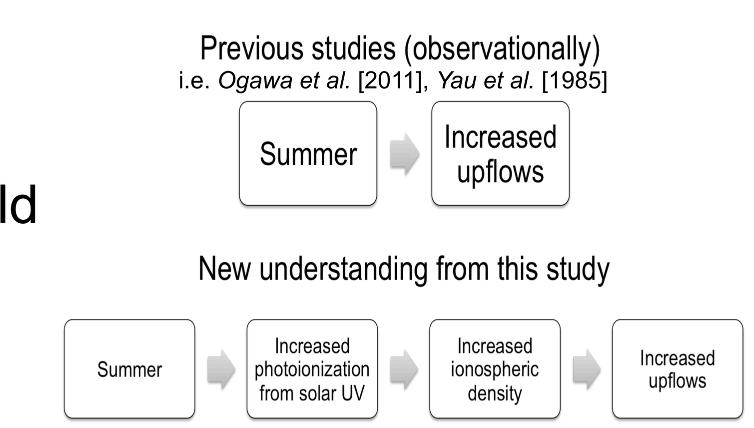

New EISCAT data from the International Polar Year (IPY) clearly shows the seasonal effect of solar UV ionization on ionospheric density, with observations that support the simulation results.

References and Acknowledgments

Lessard, M. R., Lindgren, E. A., Engebretson, M. J., and C. Weaver (2015), Solar cycle dependence of ion cyclotron wave frequencies, *Journal of Geophysical Research: Space Physics*, doi:10.1002/2014JA020791

Ogawa, Y., S. C. Buchert, I. Haggstrom, M. T. Rietveld, R. Fujii, S. Nozawa, and H. Miyaoka (2011), On the statistical relation between ion upflow and naturally enhanced ion-acoustic lines observed with the EISCAT Svalbard radar, *Journal of Geophysical Research*, 116(A03313), doi:10.1029/2010JA015827.

Strangeway, R. J., R. E. Ergun, Y.-J. Su, C. W. Carlson, and R. C. Elphic (2005), Factors controlling ionospheric outflows as observed at intermediate altitudes, Journal of Geophysical Research, 110(A03221), doi:10.1029/2004JA010829.

Varney, R. H., S. C. Solomon, and M. J. Nicolls (2014), Heating of the sunlit polar cap ionosphere by reflected photoelectrons, *Journal of Geophysical Research: Space Physics*, 119, 8660–8684, doi:10.1002/2013JA019378.

Wahlund, J.-E., H. J. Opgenoorth, I. Haggstrom, K. J. Kinser, and G. O. L. Jones (1992), EISCAT Observations of Topside Ionospheric Ion Outflows During Auroral Activity: Revisited, *Journal of Geophysical Research*, 97 (A3), 3019–3037.

Yau, A. W., P. H. Beckwith, W. K. Peterson, and E. G. Shelley (1985), Long-Term (Solar Cycle) and Seasonal Variations of Upflowing Ionospheric Ion Events at DE 1 Altitudes, Journal of Geophysical Research, 90(A7), 6395–6407.

Scan this QR Code with your mobile device for a link to the full JGR article!

Cohen et al. [2015]

EISCAT is an international association supported by research organizations in China (CRIRP), Finland (SA), Japan (NIPR and STEL), Norway (NFR), Sweden (VR), and the United Kingdom (NERC). The authors thank the EISCAT staff and several volunteers for their outstanding efforts to keep the EISCAT Svalbard Radar running during the whole International Polar Year (IPY). Funding for this research at UNH was supported by NASA grants NNX10AL17G and NNX13AJ94G and AFOSR grant FA9550-14-1-0368. R.H. Varney was supported by the Dartmouth NASA Space Grant Visiting Young Scientist Program and NSF grant AGS-1555801. The work of K. Oksavik was supported by the Research Council of Norway under contracts 212014 and 223252. The EISCAT IPY data were covered by additional funding from Norway (NFR) and the project IPY-ICESTAR.